Accepted by *Applied Physics Letters*

Diffusive Reflectance for the Free-space Light Propagation Theory

Yuanzheng Si[a)] and Heng Mao, Bin Zhang, Ming Jiang
LMAM, School of Mathematical Sciences, Peking University, Beijing 100871, China

Based on the free-space light propagation theory, the non-contact measurement technique for optical tomography provides high quality data-sets by using charge coupled device (CCD) camera for light detection. The free-space theory was originally formulated for a single object but did not take into account the reflection among object surfaces. However, complex geometries of small animals can induce multiple light reflections on surfaces. A major issue is how to model the surface reflectance to work with the free-space light propagation theory. In this letter, we utilize the Monte Carlo simulation technique to evaluate the performance of the free-space theory with multiple light reflections. Two types of surface reflectance have been simulated, including the specular or diffuse reflectance, respectively. It is found that for tissue-like objects the diffusive reflectance works the best with the free-space theory and a discrepancy occurs when the surface exhibits specular reflectance.

Biomedical optical tomography is a rapidly developing filed, which is to image the functional information of tissue abnormalities with the near-infrared light. It has been recognized as a non-invasive molecular imaging modality for its sensitivity, specificity, low-cost and non-radiation characteristics. Diffuse optical tomograph (DOT), florescence molecular tomography (FMT), and bioluminescence tomography (BLT) are several major optical tomography techniques under rapid development and intensive study.

Light migration in biological tissues is dominated by scattering for near-infrared light[1]. This results in a diffusive light emittance on the tissue surface, which is measured and then used to reconstruct the internal spatial distribution of optical properties for DOT or the light sources for BLT and FMT. For optical imaging techniques, the measurement accuracy of the light flux intensity on the tissue surface is crucial. Previous optical tomography systems utilizes fiber optic probes for the measurement, in which fibers are installed in contact with tissue. This contact approach requires that tissue be in simple shapes either by compressing or by using matching fluids. The contact approach leads to experimental inconvenience and complexity, and insufficient spatial resolution due to limited number of fibers that can be installed in practice. Using matching fluids would introduce additional photon absorption and diffusion, which reduces the signal-to-noise ratio of the measured data.

Several non-contact optical tomography systems have been reported by employing CCD cameras for light measurement[2–4]. The non-contact measurement technique (NCMT) are based on a novel theory of light propagation in free space in[4]. Combining with photogrammetric methods for obtaining arbitrary object boundaries, the non-contact measurement technique can produce high quality data sets while simplifying imaging system and experiments and has been successfully applied in FMT for both phantom and small animal experiments[5].

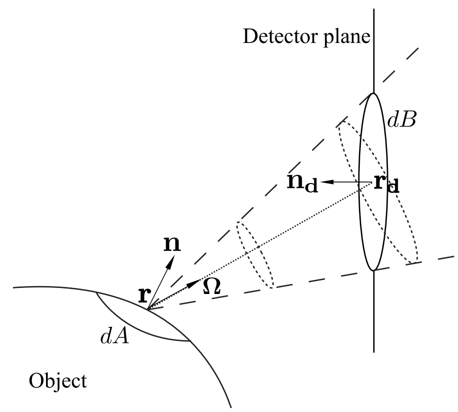

FIG. 1. Propagation of light from object surface to a virtual detector.

It is demonstrated that the non-contact measurement technique yields better image quality than traditional fiber-based methods even with a simple experimental setup[6].

The free-space theory describes the light propagation from an object surface to a CCD. It was originally for a single object but did not take into account the reflection among object surfaces in[4]. However, complex geometries of small animals can induce multiple light reflections. A major issue is how to model the surface reflectance when multiple light reflection occurs.

In this letter, we utilize the Monte Carlo simulation to evaluate the performance of the free-space theory when there sre multiple light reflections among object surfaces. Two types of surface reflectance have been simulated, including the specular or diffuse reflectance, respectively. After a number of simulations with different amount of reflections, it is found that for tissue-like objects the diffusive reflectance produces the most accurate results.

The free-space light propagation theory is briefly reviewed as follows. Consider the propagation of light from the object boundary to detector as shown in Fig. 1. Let Π be a domain in the three-dimensional Euclidean space $\boldsymbol{R}^3$ that contains the object to be imaged. Let $P(\boldsymbol{r})$ be

[a)] Correspondence to:yuanzhengsi@gmail.com

the measured light flux density at $\boldsymbol{r} \in \Gamma$, where Γ is the boundary of Π. Let $\boldsymbol{r_d}$ be a point on the detector plane. It is important to note that the "detector" plane here corresponds to the focal plane of an imaging system in practice, not the CCD sensor. Consider the energy transfer from a surface element dA at $\boldsymbol{r}$ to an element dB at $\boldsymbol{r}_d$. By the free-space theory in[4], the power emanating from dA and incident on dB is

$$P_{r \to r_d} = \frac{dB}{\pi} P(\boldsymbol{r})(\boldsymbol{n} \cdot \boldsymbol{\Omega}) \frac{\boldsymbol{n_d} \cdot (-\boldsymbol{\Omega})}{|\boldsymbol{r} - \boldsymbol{r}_d|^2} dA, \qquad (1)$$

Note that there is no numerical aperture term in the above equation because we here consider the light intensity distribution on the focal plane. In fact, there is a linear dependence between CCD measurements and the light intensity distribution on the focal plane[7]. By integrating dA over Γ, the total energy incident on dB from the object boundary can be obtained.

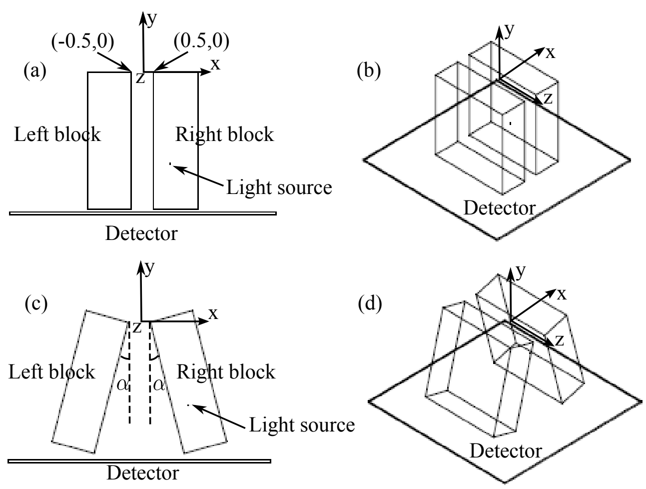

FIG. 2. Experimental setup: (a) X-Y view, (b) 3-D view, (c) X-Y view after rotating 15^o, (d) 3-D view after rotating 15^o

To study the accuracy of free-space theory when multiple reflections occur, we have designed a phantom with TracePro (Lambda Research Corporation, MA), which is a ray tracing software based on the Monte Carlo method[8]. The phantom consists of two blocks of the same size $2.0\text{mm} \times 6.0\text{mm} \times 6.0\text{mm}$, and the same tissue-like optical properties[9], their absorption coefficients $\mu_a = 0.15\text{mm}^{-1}$, scattering coefficients $\mu_s = 11.9\text{mm}^{-1}$, average cosine of the phase function $g = 0.941$, and refractive indices $n = 1.41$, for the light wavelength 630nm. The experimental setup is shown in Fig. 2. The distance between the two blocks is 1.0mm. For experimental simplicity, all the surfaces of the two blocks is set to be perfect absorber of light, except for the two surfaces facing each other. A spherical light source of radius 0.01mm, power 50mW and wavelength 630nm, is placed at $(1.25\text{mm}, -4\text{mm}, 0)$ inside the right block. A virtual detector of size $12\text{mm} \times 12\text{mm}$ is placed 1mm below the two blocks to simulate the focus plane of CCD cameras. The angle between the two blocks is altered to adjust the amount of light reflectance in the following. In our simulation, the left block is rotated α degrees in the clockwise direction around the line $(x = -0.5\text{mm}, y = 0\text{mm})$, while the right block is rotated counter-clockwise around the line $(x = 0.5\text{mm}, y = 0\text{mm})$. Fig.2(c) and Fig.2(d) show the experimental setup with $\alpha = 15°$.

We have performed a number of Monte Carlo simulations at $\alpha = 0°, 15°, 30°$ when the two facing surfaces are set first to be specular and then diffusive, respectively, in our simulation. For the specular reflectance setting, the law of reflection was used to model the specular reflection. For the diffusive reflectance setting, we use the Lambertian model for diffuse reflection in which light is reflected with equal radiance in all directions. At most 1×10^9 photons were traced at each angle to ensure the accuracy of Monte Carlo simulations. The detector plane is discretized into 256×256 rectangular pixels.

The intensity distribution on the detector by Monte Carlo simulation is collected and then compared with the intensity distribution computed from the free-space theory. To compute the intensity distribution on the detector by the free-space theory by Eq. (1), we need to know the light flux on the two facing surfaces. This is obtained by collecting the outward light flux on the two surfaces during Monte Carlo simulations, which can be experimentally done only with Monte Carlo simulation. For comparison, the following relative error is computed, $E_{\text{rel}} = 1/T \sum_{p(i,j)>0} |y(i,j) - p(i,j)|/p(i,j)$, where $y(i,j)$ is the light intensity computed by the free-space theory at pixel (i,j), and $p(i,j)$ the simulated data at pixel (i,j). T is the number of pixels at which the simulated light distribution $p(i,j)$ is non-zero.

At each angle $\alpha = 0°, 15°, 30°$, the two facing surfaces are set to first exhibit specular reflectance and then diffuse reflectance. We then compare the relative error for both cases to evaluate how different types of reflection affect the accuracy of free-space theory. Fig. 3 shows a comparison of the relative errors versus the increasing number of photons with $\alpha = 0°, 15°, 30°$, respectively. When the photon number is 1×10^9, the relative errors for the specular reflectance are $0.35, 0.18, 0.12$, respectively, for $\alpha = 10°, 15°, 30°$, and the relative errors for the diffusive reflectance are $0.07, 0.04, 0.02$, respectively. The relative error in the specular case is an order of magnitude higher than that of the diffusive case. Fig. 3 also demonstrates that the relative error decreases when α increases. This is because the larger α is, the greater the amount of reflectance. This implies that the accuracy of free-space theory is not only affected by the types of reflectance, but also the amount of reflection.

Fig. 4 and Fig. 5 are representative profiles of the normalized intensity distributions on the detector at the 64th and 128th horizontal line, respectively, from the free-space theory and from the Monte Carlo simulation. It follows that the results from the free-space theory agree quite well with the Monte Carlo simulations if the reflectance is diffusive. A discrepancy occurs if the re-

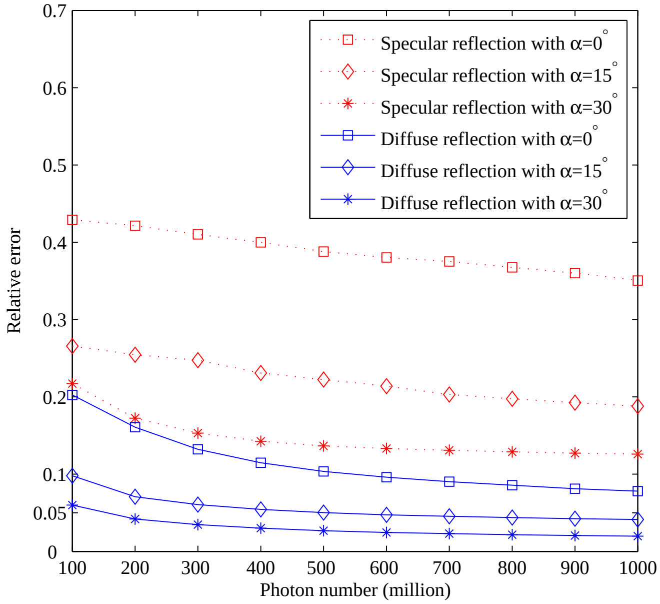

FIG. 3. Relative errors between the result from free-space theory and Monte Carlo simulations for diffuse and specular reflectance, respectively, when $\alpha = 0°, 15°, 30°$.

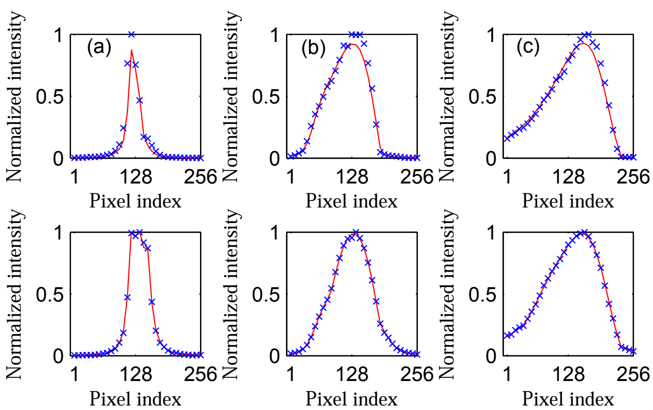

FIG. 4. Profiles of the normalized intensities at the detector for the free-space theory (red solid line) and Monte Carlo simulation (blue cross)) at the 64th row for the specular reflectance (top) and diffusive reflectance (bottom), respectively, when (a) $\alpha = 0°$, (b) $\alpha = 15°$, and (c) $\alpha = 30°$.

flectance is specular. This discrepancy decreases when the angle between the two blocks increases.

In our simulation, the maximum absolute error in the specular reflectance case is 1.7×10^{-5} mW per pixel. If we assume a 50ms exposure time, the error is approximately equal to the power of 2.6×10^8 photons (630nm), which can detected by modern scientific CCD cameras.

In conclusion, we have preformed Monte Carlo simulations to evaluate the performance of the free-space light propagation theory in the presence of multiple light reflections among object surfaces for tissue-like objects. Two types of surface reflectance have been simulated, in-

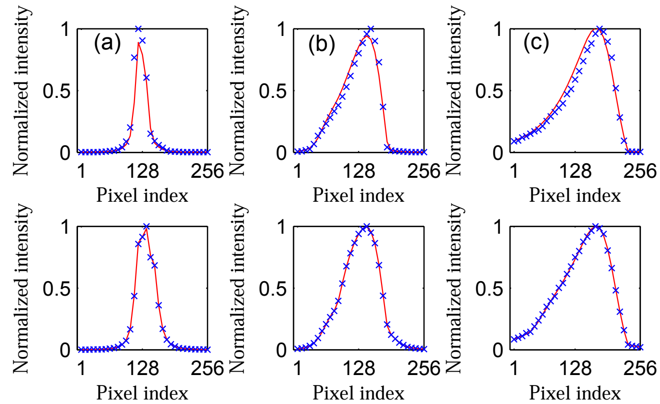

FIG. 5. Profiles of the normalized intensities at the detector for the free-space theory (red solid line) and Monte Carlo simulation (blue cross)) at the 128th row for the specular reflectance (top) and diffusive reflectance (bottom), respectively, when (a) $\alpha = 0°$, (b) $\alpha = 15°$, and (c) $\alpha = 30°$.

cluding the specular or diffuse reflectance, respectively. We also study the effect of reflectance amount. When the surface is diffusive, the free-space theory agrees quite well with the Monte Carlo simulations. However, a discrepancy occurs when the surface exhibits specular reflectance. Because this discrepancy can be detected by modern scientific CCD cameras, the diffusive reflectance of object surfaces is recommended for optical tomography of small animals.

This work is supported in part by NSFC grants (60325101, 60628102, 60872078) and MSRA.

[1] S. R. Arridge, Inverse Prob. **15**, R41–R93 (1999).
[2] Ignacio Iglesias and Jorge Ripoll, J. Biomed. Opt. **14**, 024003–7 (2009).
[3] N. Deliolanis, T. Lasser, D. Hyde, A. Soubret, J. Ripoll, and V. Ntziachristos, Opt. Lett. **32**, 382–384 (2007).
[4] Jorge Ripoll, Ralf B. Schulz, and Vasilis Ntziachristos, Phys. Rev. Lett. **91**, 103901 (2003).
[5] Ralf B. Schulz, Jorge Ripoll, and Vasilis Ntziachristos, Opt. Lett. **28**, 1701–1703 (2003).
[6] Ralf B. Schulz, Jorg Peter, Wolfhard Semmler, Cosimo D'Andrea, Gianluca Valentini, and Rinaldo Cubeddu, Opt. Lett. **31**, 769–771 (2006).
[7] J. Ripoll and V. Ntziachristos, Mod. Phys. Lett. B **18**, 1403–1431 (2004).
[8] L. H. Wang, S. L. Jacques, and L. Q. Zheng, Comput. Meth. Prog. Biomed. **47**, 131–146 (1995).
[9] W. F. Cheong, S. A. Prahl, and A. J. Welch, IEEE J. Quantum Elect. **26**, 2166 – 2185 (December 1990).